Available online at www.sciencedirect.com
SCIENCE DIRECT®
Physica B 343 (2004) 216–221
PHYSICA B
www.elsevier.com/locate/physb

A test bed for a finite-difference time domain micromagnetic program with eddy currents

L. Yanik[a], E. Della Torre[a,b,*], M.J. Donahue[b]

[a] *Institute for Magnetics Research, The George Washington University, Washington, DC 20052, USA*
[b] *National Institute of Standards and Technology, Gaithersburg, MD 20899, USA*

Abstract

The inclusion of eddy currents into micromagnetic programs is important for the proper analysis of dynamic effects in conducting magnetic media. This subject has received little attention in the past although it can cause significant errors in device calculations. This paper introduces a computational test bed for eddy current calculations and discusses some interesting analytic cases in this simplified geometry.

PACS: 83.60.Np; 75.40.Mg; 85.70.Ay

Keywords: Eddy current; Micromagnetics; FDTD

1. Introduction

An approach to the solution of micromagnetic problems with eddy currents has been proposed [1] and implemented [2]. This approach requires the simultaneous solution of the coupled equation for eddy currents and for magnetization evolution. In this paper, we present a program using finite-difference time domain, FDTD, calculations for a simplified problem to be used as a test bed for more general programs. It is our intention to use this program to verify the accuracy of more general programs in these test cases, and also to present some results that we will use to test the final model.

The problem with introducing eddy currents into a micromagnetic calculation is that the changing magnetization induces an electric field in the material which produces the eddy currents. Since the eddy currents are bound by the shape of the material, the induced electric field has to be tangential to the boundary at all points on the boundary. This requires surface charges to be induced to steer the currents within the material. To avoid the computation of these currents, in this model we have chosen a circular cylinder that, by symmetry, naturally forces the electric field to be tangential to the boundary. Also, the symmetry of this geometry permits the computed quantities to vary only with the radial coordinate.

*Corresponding author. Institute for Magnetics Research, The George Washington University, Washington, DC 20052, USA. Tel.: +1-202-994-0410; fax: +1-202-994-0227.
E-mail address: edt@gwu.edu (E. Della Torre).

0921-4526/$ - see front matter
doi:10.1016/j.physb.2003.08.097

2. The model

We developed a model for an infinite circular cylinder of radius R, consisting of a perfect crystal of uniaxial material whose easy axis, z, coincides with the cylinder's axis, as shown in Fig. 1. The initial condition that we will assume is uniform magnetization in the negative z-direction. If we apply a field in the z-direction, the magnetization will attempt to reverse. In order to break the radial symmetry, we will offset the magnetization at the surface by a fraction of a degree, δ, which will nucleate a Bloch wall at the surface that will start propagating inwards towards the center, and eventually annihilate itself at the axis. The moving wall will induce eddy currents that impede the wall's progress.

Due to the symmetry of this configuration, we expect the magnetization to change but remain cylindrically symmetric. We elected to overlay a Cartesian coordinate system on the cross section of the cylinder, as illustrated in Fig. 2. Only the node values on the central row of the computational grid are calculated by FDTD. The node values for the row above and the row below the computation row are obtained by interpolating appropriate points on the center row and rotating them to the adjacent rows. We note that there is a singularity at the center of the cylinder, which presents problems when trying to reverse the magnetization completely. The choice of this coordinate system of calculation rather than the more obvious cylindrical coordinate system was motivated by the ease of generalizing these calculations later to arbitrary shapes.

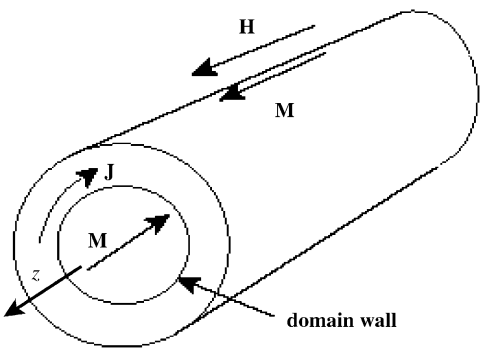

Fig. 1. Cylinder's geometry.

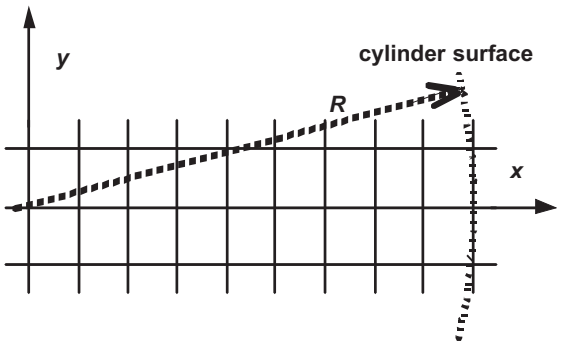

Fig. 2. Computational grid used in the model.

The magnetization could be computed by either applying the Landau–Lifshitz–Gilbert equation, to study high-speed phenomena, or by minimizing the energy of the system at each calculation step. In this calculation, due to the symmetry just discussed, we assume that the magnetization lies in the y–z plane, so that only Bloch-type walls may be formed. This rules out the possibility of precessing spins; so we are forced to use the energy-minimization approach limiting calculations to relatively slow variations of the applied field compared to magnetization changes.

Under the above assumptions, the magnetization will be of the form

$$\mathbf{M}(r) = M_S(\cos\alpha\,\mathbf{1}_z + \sin\alpha\,\mathbf{1}_y), \tag{1}$$

where $\alpha(r)$ is the angle that the magnetization makes with respect to the z-axis. With this magnetization pattern, there are no demagnetizing fields. If the applied field and, consequently, the magnetization change with time, an electric field will be induced. By Faraday's law, the curl of that field is given by

$$\operatorname{curl}\mathbf{E} = -\frac{\partial\mathbf{B}}{\partial t} = \mu_0\left(\frac{\partial\mathbf{H}}{\partial t} + \frac{\partial\mathbf{M}}{\partial t}\right). \tag{2}$$

The z component of the electric field is limited to the wall region and generates two oppositely directed currents. Hence, these currents will generate a small magnetic field which dies off quickly with distance. Therefore, neglecting the z

component, the electric field is given by

$$\mathbf{E}(r) = -\frac{\mu_0 \mathbf{1}_y}{r}\int_0^r \left[\frac{\partial H_z(\rho,t)}{\partial t} + \frac{\partial M_z(\rho,t)}{\partial t}\right]\rho \, \mathrm{d}\rho. \quad (3)$$

This electric field will induce the eddy currents. If the time scale is appropriate, then these currents can be computed using Ohm's law $\mathbf{J} = \sigma \mathbf{E}$. By Ampere's law, the field in the interior of the material will differ from the surface field by the eddy currents. Thus, the field at any point, $H_z(r)$ is given by

$$H_z(r) = H_{\mathrm{app}} + \int_r^R J_y \, \mathrm{d}\rho, \quad (4)$$

where $H_z(R) = H_{\mathrm{app}}$ is the field at the surface.

The magnetization is computed by assuming that the magnetization patterns are a sequence of equilibrium states that minimize the total energy in the current local field. The applied field is assumed to be the sum of the applied field and the field due to the eddy currents. The total energy is the sum of the exchange energy, the anisotropy energy and the Zeeman energy. The exchange energy per unit computational cell is

$$w_{\mathrm{ex}} = -\frac{A\mathbf{M}\cdot\nabla^2\mathbf{M}}{M_S^2} \approx \frac{A(6M^2 - \mathbf{M}\cdot\Sigma\mathbf{M})}{M_S^2 h^2}, \quad (5)$$

where h is the distance between nodes in the grid and Σ indicates a sum over the six nearest neighbor nodes. The anisotropy energy for uniaxial anisotropy is

$$w_{\mathrm{anis}} = K \sin^2\alpha. \quad (6)$$

Finally, the Zeeman energy is given by

$$w_{\mathrm{Zeeman}} = -\mu_0 H_z(r) M_z(r) - \mu_0 M_S H_z(r)\cos[\alpha(r)]. \quad (7)$$

In the program, at each time step the magnetization pattern is computed by varying $\alpha(r)$ at each node using the current value of H, then computing the change in magnetization so that the electric field can be computed using Eq. (3). With this electric field, the eddy currents are computed and H is recomputed using Eq. (4). This procedure is repeated until H converges. Then we proceed to the next time step and continue until finished. A flow chart of this process is shown in Fig. 3.

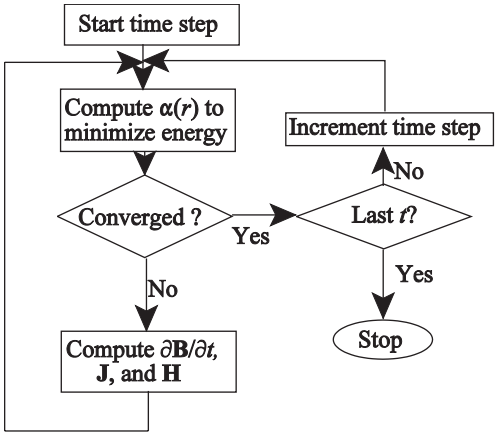

Fig. 3. Flow chart of calculation.

This problem is defined by the material parameters: A, K, and M_S, the geometric parameter R and the applied field as a function of time. Instead of K and A, we prefer to use the domain wall width of a planar Bloch wall, l_w,

$$l_w = \pi\sqrt{\frac{A}{K}} \quad (8)$$

and the wall energy density w_w per unit area of a planar Bloch wall

$$w_w = 4\sqrt{AK}. \quad (9)$$

In the solutions that we obtained even though the walls were Bloch-type, since the domain wall had curvature, neither the wall width nor the energy density were equal to these values.

3. An analytical example

There are some cases where an analytical solution can be obtained. If l_w is negligible compared to $r_w < R$, then the problem reduces to a domain level problem. Furthermore, we can neglect the effect of wall curvature on both l_w and w_w. Then the problem has a single unknown, the radius, r_w, of the wall, and the magnetization changes when the wall moves. From Faraday's law, assuming that $M_S \gg H$, the line integral of the electric field around any circle, C, centered on the

z-axis using Eq. (2) is

$$\oint_C \mathbf{E}\cdot\mathbf{dl} = \begin{cases} 4\pi\mu_0 M_S v r_w & \text{if } r > r_w, \\ 0 & \text{if } r < r_w, \end{cases} \tag{10}$$

where v is the velocity of the domain wall. Hence, the current density is given by

$$\mathbf{J} = \begin{cases} \dfrac{2\sigma\mu_0 M_S v r_w}{r}\mathbf{1}_y & \text{if } r > r_w, \\ 0 & \text{if } r < r_w. \end{cases} \tag{11}$$

The field at the wall from Eq. (4) is

$$\mathbf{H}(r_w) = \left[H_{app} - \int_R^{r_w} \frac{2\sigma\mu_0 M_S v r_w}{r}\,dr\right]\mathbf{1}_z = \left[H_{app} + 2\sigma\mu_0 M_S v r_w \ln(R/r_w)\right]\mathbf{1}_z. \tag{12}$$

We have thus far not discussed any dynamics of the wall. For a perfect crystal, the critical field is negligible and for relatively slow magnetizing processes, we can neglect the wall mass. Then, we can set the field in Eq. (12) equal to zero and solve for the wall's velocity

$$0 = \left[H_{app} + 2\sigma\mu_0 M_S v r_w \ln(R/r_w)\right] \tag{13}$$

or

$$v = -\frac{H_{app}}{2\sigma\mu_0 M_S r_w \ln(R/r_w)}. \tag{14}$$

We see that as the wall moves closer towards the center, it has to speed up if the applied field remains the same. Fig. 4 is a plot of the position of the domain wall as a function of time for a constant positive applied field. Cutting the conductivity or the saturation magnetization into half, or doubling the applied field, all have the effect of doubling the velocity and cutting the reversal time into half. Note that the slope of the wall's position diverges as the wall approaches the center. A plot of the normalized magnetization of the cylinder is shown in Fig. 5.

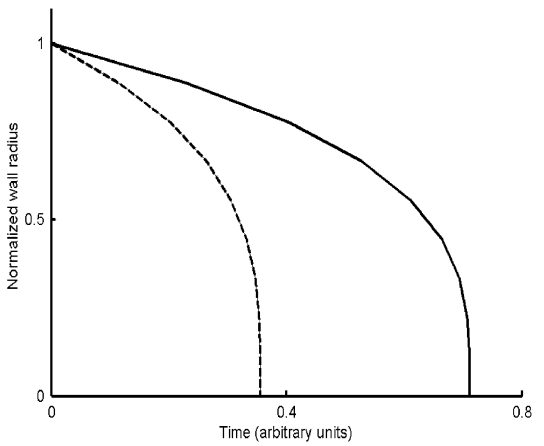

Fig. 4. A plot of the wall's position as a function of time for a constant applied field. The dotted line shows the effect of cutting the conductivity in half.

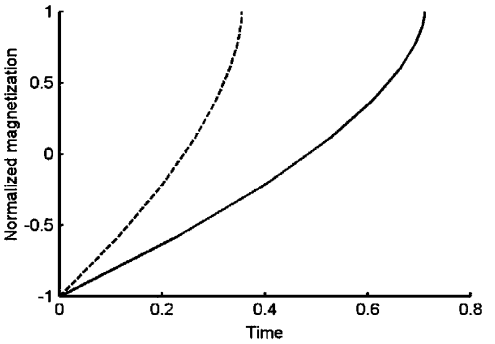

Fig. 5. Normalized magnetization in the cylinder as a function of time for a constant applied field. The dotted line shows the effect of cutting the conductivity into half.

In the simplified model, we can include a finite critical field by requiring that the field at the wall be equal to the critical field if the wall is to move. That is

$$v = \begin{cases} -\dfrac{H_{app} - H_C}{2\sigma\mu_0 M_S r_w \ln(R/r_w)} & \text{if } H_{app} > H_C, \\ 0 & \text{if } H_{app} < H_C. \end{cases} \tag{15}$$

It is more difficult to include wall mass into these calculations. This mass includes the effect that when the wall moves, the spins have to rotate [3] and becomes important at higher speed applications.

The effect of the wall energy in this model is to produce an effective field, H_w, tending to push the wall towards the center. This is due to the fact that the total wall energy per unit length, W_w, is directly proportional to the length of the circumference of the wall:

$$W_w = 2\pi r_w w_w, \tag{16}$$

So that

$$H_w = \frac{1}{\mu_0 M_S}\frac{dW_w}{dr_w} = \frac{2\pi w_w}{\mu_0 M_S} + \frac{2\pi r_w\, dw_w}{\mu_0 M_S\, dr_w}. \quad (17)$$

Even if there is no applied field but the wall energy is uniform, if $H_w > H_C$, then the wall will shrink to the center as was observed in iron single crystals [3].

If we apply a ripple to the wall energy such as

$$w_w = w_0 + \Delta w \sin(\beta r_w), \quad (18)$$

then we can simulate a critical field. When the wavelength of the ripple, $2\pi/\beta$, is much larger than the wall width, the peak value of dw_w/dr_w will be $\beta\,\Delta w$. Thus, in order to keep the wall propagating, the field at the wall will have to be greater than $\beta\,\Delta w$. We have created an effective critical field of $\beta\,\Delta w$. For smaller fields, the wall can hang up at periodic points that are separated by $2\pi/\beta$.

For a very short wavelength ripple, the wall energy will be integrated over the ripple and since the average value of sin x over a period is zero, there will be no critical field. If one assumes an equal angle model wall such as

$$\alpha = \begin{cases} 0 & \text{if } r > r_w + l_w/2, \\ 2\pi(r_w - r)/l_w & \text{if } |r - r_w| < l_w/2, \\ \pi & \text{if } r < r_w - l_w/2, \end{cases} \quad (19)$$

then one can compute the critical field as a function of wall width. In particular, in this case the rate of change of α with r is constant, so the average critical field over the wall is

$$\langle H_C \rangle = \left| \frac{\Delta w}{l} \int_{-l/2}^{l/2} \cos(\beta r)\, dr \right| = \left| \frac{2\Delta w}{\beta l} \sin\frac{\beta l}{2} \right|. \quad (20)$$

A plot of the variation in critical field, normalized to the zero thickness wall, with wall width normalized to β, is shown in Fig. 6. It is seen that when the wall width is an integer multiple of β, the critical field goes to zero.

When the applied field is reversed, there are two possibilities: the wall could reverse direction or a new wall could be nucleated at the surface and start propagating inward. The choice of which occurs is determined by the size of the nucleating field compared to the size of the propagating field. In the analytical example, we simply postulate that there is no wall until an arbitrary nucleating field is reached. If that field is small enough, there is the possibility that there may be more than one wall active at any time. However, the outermost wall will see the largest field since the inner walls will have additional shielding by the eddy currents between the walls. Thus, as long as the critical field is uniform over the cylinder, we can assume that we have a single wall active at any time.

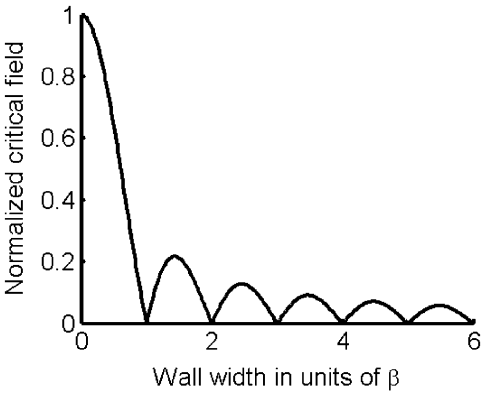

Fig. 6. Variation of the critical field with wall thickness.

In the numerical example, we controlled the size of the nucleating field by the size of δ at the surface layer. The larger the δ, the smaller the nucleating field. The propagating field is controlled by the critical field and the wall mass. In the present numerical model, there is no critical field. Also, there is no wall mass, since we have not included dynamics in the propagation of the domain wall.

4. Energy considerations

There are two processes that dissipate power in this model: hysteresis and eddy current losses. The hysteresis loss per unit length is given by

$$w_{hyst} = \int_0^R 2\pi r \mu_0 H_C \frac{\partial M}{\partial t}\, dr. \quad (21)$$

For the thin wall with a constant applied field, this reduces to

$$w_{\mathrm{hyst}} = 4\pi r \mu_0 H_{\mathrm{C}} M_{\mathrm{S}} v. \tag{22}$$

The eddy current loss per unit length is given by

$$w_{\mathrm{ec}} = \int_0^R 2\pi\sigma J^2 r \, \mathrm{d}r. \tag{23}$$

For a thin wall with a constant applied field, this reduces to

$$w_{\mathrm{ec}} = \int_{r_{\mathrm{w}}}^R 2\pi\sigma r \left(\frac{2\sigma\mu_0 M_{\mathrm{S}} v r_{\mathrm{w}}}{r}\right)^2 \mathrm{d}r$$
$$= 8\pi\sigma^3 \left(\mu_0 M_{\mathrm{S}} v r_{\mathrm{w}}\right)^2 \ln(R/r_{\mathrm{w}}). \tag{24}$$

We note that in this equation, both v and r_w are functions of time, even if the applied field is held constant. This may be further reduced using Eq. (12) if desired.

5. Conclusions

We have presented a simplified model of the introduction of eddy currents into a micromagnetic calculation. We also discussed the special analytic calculation in the case of a thin domain wall. This paper is intended to provide a limiting calculation to test a more general model.

Acknowledgements

This work was supported by a grant from the Department of Commerce through the National Institute of Standards and Technology.

References

[1] E. Della Torre, J.G. Eicke, IEEE Trans. Magn. 33 (1997) 1251.
[2] L. Torres, L. Lopez-Diaz, E. Martrinez, O. Alejos, Micromagnetic dynamic computations including eddy currents, INTERMAG Conference, Boston, MA, paper CA-01, 2003.
[3] J.K. Galt, J. Andrus, H.G. Hopper, Rev. Mod. Phys. 25 (1953) 93.